

Virgin effect in spheres of LaFeSi-based alloys

Cite as: AIP Advances **12**, 065216 (2022); <https://doi.org/10.1063/5.0093772>

Submitted: 06 April 2022 • Accepted: 24 May 2022 • Published Online: 17 June 2022

 Christian R. H. Bahl,  Jierong Liang,  Marvin Masche, et al.



View Online



Export Citation



CrossMark

ARTICLES YOU MAY BE INTERESTED IN

[Optical measurements on a budget: A 3D-printed ellipsometer](#)

American Journal of Physics **90**, 445 (2022); <https://doi.org/10.1119/10.0009665>

[How much gallium do we need for a p-type Cu\(In,Ga\)Se₂?](#)

APL Materials **10**, 061108 (2022); <https://doi.org/10.1063/5.0091676>

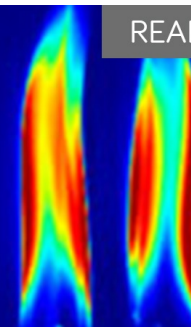
[An improved acoustic imaging algorithm combining object detection and beamforming for acoustic camera](#)

JASA Express Letters **2**, 064802 (2022); <https://doi.org/10.1121/10.0011735>

AIP Advances

Fluids and Plasmas Collection

READ NOW



Virgin effect in spheres of LaFeSi-based alloys

Cite as: AIP Advances 12, 065216 (2022); doi: 10.1063/5.0093772

Submitted: 6 April 2022 • Accepted: 24 May 2022 •

Published Online: 17 June 2022



Christian R. H. Bahl,^{1,a)}  Jierong Liang,^{1,2}  Marvin Masche,¹  Kaspar K. Nielsen,^{1,b)} 
and Kurt Engelbrecht¹ 

AFFILIATIONS

¹ Department of Energy Conversion and Storage, Technical University of Denmark, Fysikvej 310, DK 2800 Kgs. Lyngby, Denmark

² Section of Thermal Energy, Department of Mechanical Engineering, Technical University of Denmark, Koppels Alle 403, DK 2800, Kgs. Lyngby, Denmark

^{a)} Author to whom correspondence should be addressed: chr@dtu.dk

^{b)} Presently at: BEC Financial Technologies, Havsteensvej 4, 4000 Roskilde, Denmark.

ABSTRACT

A virgin phase transition is observed in spherical particles of the industrially relevant magnetocaloric material $\text{La}(\text{Fe},\text{Mn},\text{Si})_{13}\text{H}_y$. Upon initial cooling, the phase transition is observed 2–3 K below the heating transition on all subsequent cooling and heating transitions. This virgin transition has been studied using differential scanning calorimetry and vibrating sample magnetometry. Incremental measurements show not only how the phase transition can be carefully approached but also that the initial full transformation requires cooling of about 6 K below the observed phase transformation. No signs of structural damage due to the thermal cycling were observed, neither macroscopically or by scanning electron microscopy.

© 2022 Author(s). All article content, except where otherwise noted, is licensed under a Creative Commons Attribution (CC BY) license (<http://creativecommons.org/licenses/by/4.0/>). <https://doi.org/10.1063/5.0093772>

I. INTRODUCTION

The technology of magnetic refrigeration is evolving, and devices presented in the literature are getting more powerful and efficient.^{1,2} The technology is based on the magnetocaloric effect, where the temperature of a material increases or decreases when a magnetic field is applied or removed, respectively. When a structural and a magnetic phase transition coincide, the material is said to have a first-order magnetic phase transition. This is often referred to as a first-order material, as opposed to materials with purely magnetic transitions, which are known as second-order ones.³ Such first-order materials are interesting for magnetic refrigeration as the steep change in magnetization at the phase transition will result in a very high isothermal entropy change. However, the range of the useful magnetocaloric effect is in general very narrow, only about 3–5 K,³ in the applied magnetic fields relevant for devices (~1 T). This issue has been circumvented by layering materials with a slight change in the transition temperature, T_t , from layer to layer, see, e.g., Ref. 4. In this way, the full designed operating range of the regenerator can be covered. It has been shown how the performance of a device with layered magnetocaloric materials is very sensitive to the temperature spacing between the layers, but critically also to the systematic spacing of the individual transition temperatures.⁵ Thus,

in the design phase, accurate knowledge of the transition temperature of each layer is important. Likewise, it is equally important that this series of transition temperatures is actually realized during the construction of the final device.

The material family $\text{La}(\text{Fe},\text{Si})_{13}$ has become one of the most popular families to use in devices and prototypes.^{2,4,6–8} The as-prepared transition temperatures of this material family are around 200 K.^{9,10} When interstitial hydrogen is added, the transition temperature can be tailored in a broad range around room temperature, but actual control can be challenging due to the requirement of accurate hydrogenation.¹¹ When fully hydrogenated, substituting some Fe with Mn allows fine tuning of the transition temperature.¹² However, the inclusion of hydrogen generally increases the brittleness of the material, making shaping a challenge.

Waske *et al.*¹³ studied the transition in an unhydrogenated $\text{La}(\text{Fe},\text{Si})_{13}$ material with a first order transition. They found slightly different behavior during both first cooling and first heating cycles, compared to subsequent cycles. This was observed in the form of broadened transitions, of the order of 0.5 K, but without temperature shifting. The changes were ascribed to pressures in the structure being released, causing cracks and finally breaking of the sample. Similar indications of constrained structures were observed by Neves Bez *et al.*¹⁴

Virgin transitions have previously been observed in the Fe_2P type system,^{15,16} which is also considered for room temperature magnetic refrigeration. Specifically in $(\text{Mn,Fe})_2(\text{P,Si})$, several studies have shown a delayed transition, far below the cycled one (10–20 K). This has been ascribed to the volume change of the material being hindered by the structure¹⁷ or to the presence of a metastable state originating during high temperature processing.¹⁵ A study showed how it was possible to regain the virgin transition by annealing to thermally reset the sample.¹⁵ Typically, severe cracking is observed after the first phase transition, often leading to sample breaking.^{16,17}

In the following, we will report on the presence of a virgin transition at a reduced temperature in $\text{La}(\text{Fe,Mn,Si})_{13}\text{H}_y$, which has not been previously reported. We will also show how, due to the resilience of the material structure, this transition does not affect the structure or stability of the samples. This makes them suitable as magnetocaloric materials in future devices.

II. EXPERIMENTAL

A. Materials

Nearly spherical particles of $\text{La}(\text{Fe,Mn,Si})_{13}\text{H}_y$ were produced by Vacuumschmelze GmbH & Co. KG, Hanau, Germany, as described in Ref. 7. The feed-stock material was extruded, cut into pieces, and mechanically spheronised to near sphere shaped particles. Several versions of this material, known as CALORIVAC, are available and have been previously studied. In the present version, the structure has been stabilized by the inclusion of α -Fe in the structure, and it is known as CALORIVAC-HS. The material has been previously shown to be of first order but with negligible hysteresis.¹⁸ The temperature of the transition between the ferromagnetic and paramagnetic phases is controlled by varying the Mn and Si content. A series of ten alloys was obtained, spanning a range of transition temperatures of 20 K, from 292 K and down. The alloys were used in a magnetocaloric heat pump recently constructed at DTU Energy.² Two samples were chosen for the study presented here: sample A ($\text{LaFe}_{11.18}\text{Mn}_{0.45}\text{Si}_{1.37}$)₁₃H_y, with a T_t of 290.1 K, and sample B ($\text{LaFe}_{11.07}\text{Mn}_{0.56}\text{Si}_{1.37}$)₁₃H_y with a T_t of 273.1 K; both temperatures were measured using a zero field differential scanning calorimeter (DSC). Both samples are hydrogenated to saturation, with a y of about 1.65. The indicated compositions are nominal.

B. Differential scanning calorimeter

A DSC, custom built at DTU Energy, was used to characterize the specific heat of the samples. Details of the instrument can be found in Ref. 19. The temperature can be varied in the range 230–330 K. A magnetic field can be accurately applied and continuously varied in the range of 0–1.5 T. This makes it possible to fully characterize room temperature magnetocaloric materials in the relevant temperature and magnetic field ranges. In addition, the DSC also has a very fine temperature control, ensuring that there is negligible overshoot of temperatures during ramping. The DSC can operate with very low temperature ramp rates, giving a high temporal and thus thermal resolution, which allows observation of very fine details.²⁰ There is, however, a trade-off as the signal is proportional to the ramp rate. A low ramp rate can result in a noisy signal.

All data presented here were collected at temperature ramp rates of ± 0.5 K/min or ± 1 K/min.

C. Vibrating sample magnetometer (VSM)

A commercial Lake Shore 7407 vibrating sample magnetometer (VSM) was used to measure the magnetic properties of the samples in the field range of 0–1.5 T. It was equipped with a cryostat cooled by liquid nitrogen, allowing accurate temperature control during measurements in the relevant range. Temperature ramping was very slow in order to avoid any overshooting while approaching a new temperature set point.

III. RESULTS AND DISCUSSION

As shown in Fig. 1, a sample consisting of 15 spheres of sample A (equivalent to 13.63 mg) has been measured in the DSC in different magnetic fields, as indicated. As shown in Fig. 1(a), each line shows the specific heat capacity during cooling, starting from high temperature. The measurements are made in an order, starting from the lowest field (0.03 T) and ending with the highest (1.36 T). Figure 1(b) shows the specific heat capacity during heating, starting from low temperature. Again, the measurements are made in an order, starting from the lowest field and ending with the highest. Figures 1(c) and 1(d) show selected data from repeats of the experiments in Figs. 1(a) and 1(b). It is clearly observed that the first measurement at 0.03 T in Fig. 1(a) is different from the others. The signal is more clearly split into several peaks and at a lower temperature than expected when extrapolating the series of peaks in other applied fields. During heating, as shown in Fig. 1(b), just a single peak with some shoulders is observed at the temperature where it would be expected. The repeat measurements in Figs. 1(c) and 1(d) are consistent with the initial heating data. The slight difference in the peak temperatures between the heating and cooling data is due to a slight lag in the temperature during ramping. Extrapolating this shift from data recorded at other ramp rates indicates a negligible hysteresis.

The peaks of the heat capacity are sharp and shift to higher temperatures when a magnetic field is applied, indicating first-order properties. However, the lack of hysteresis and the relatively fast decline in peak amplitude of the specific heat in applied magnetic fields indicate that it is very close to being a second-order transition.

A single sphere of sample A was measured in the VSM in an applied field of $\mu_0 H = 10$ mT. The sphere was measured twice from 320 K down to 260 K and back up to 320 K, in 1 K intervals. Figure 2 shows how there is, again, a different behavior in the first cooling, with a lower transition temperature. Subsequent cooling and heating curves are remarkably similar, confirming the absence of hysteresis at the phase transition of this sample.

The same lower transition temperature upon cooling is also observed in sample B. Figure 3 shows the results obtained when cooling and heating a sample of about 100 spheres from 310 to 250 K and back. Again, the second cooling is remarkably similar to the heating. It is clear from the results in Figs. 1–3 that the samples experience a different transition in the first cooling, a so-called virgin transition. The measured transition temperatures are given in Table I.

In order to further study the nature of the phase transition, a single sphere of sample B was cooled from room temperature to

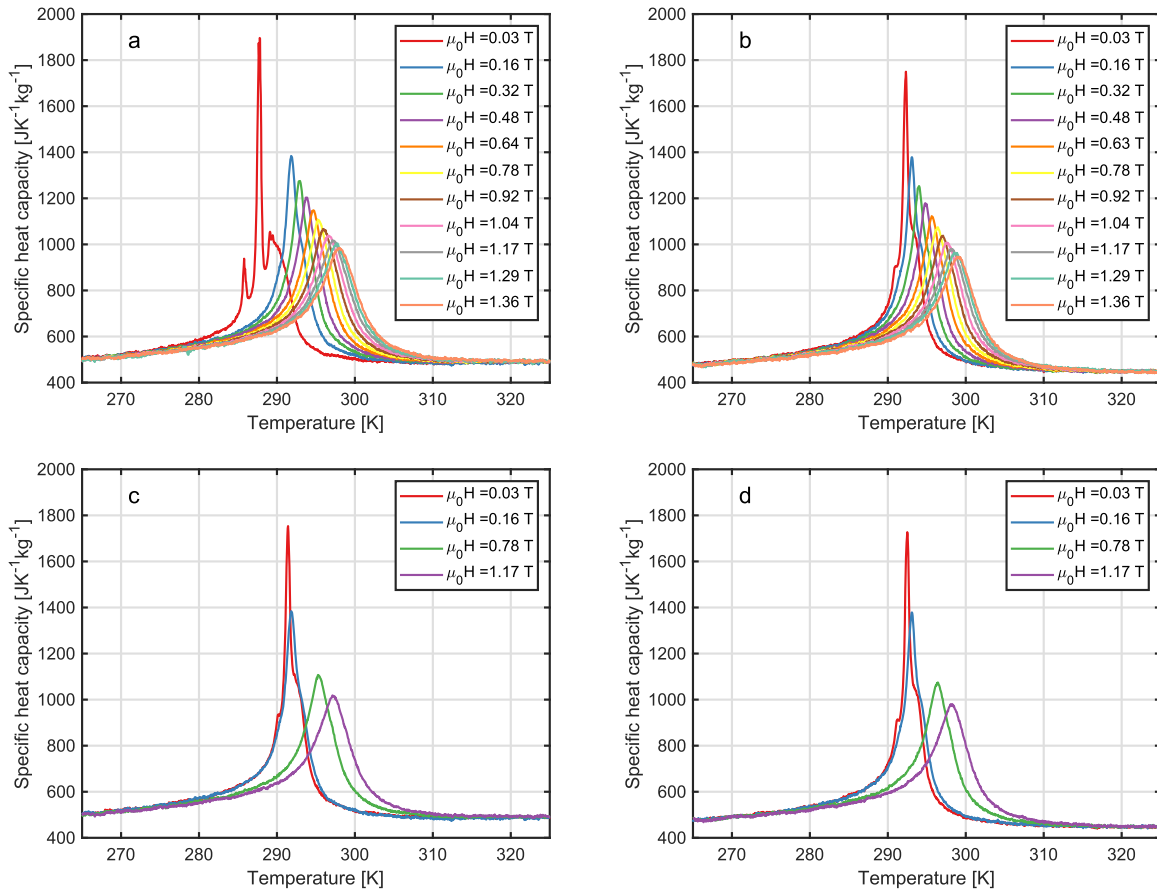


FIG. 1. Specific heat capacity of sample A in different applied magnetic fields, as indicated by the legend. (a) First cooling. (b) First heating. (c) Second cooling. (d) Second heating. All the data are collected at a ramp rate of ± 1 K/min.

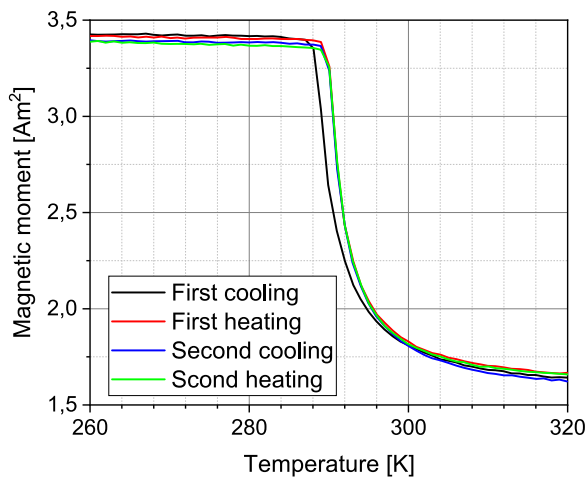


FIG. 2. VSM measurements of a single sphere of sample A in an applied field of $\mu_0 H = 10$ mT.

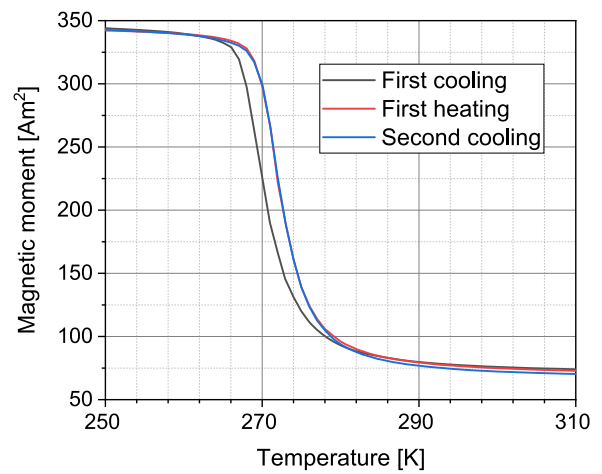


FIG. 3. VSM measurements of an ensemble of spheres of sample B in an applied field of $\mu_0 H = 10$ mT.

TABLE I. Measured transition temperatures during first and second heating and cooling experiments. For the DSC data, the temperature of the highest peak is used as the transition temperature. For the VSM data, the inflection point of the magnetization data is used to determine the transition. As the temperature step in the VSM data is 1 K, the value is given at this resolution.

Sample	First cooling (K)	First heating (K)	Second cooling (K)	Second heating (K)
A (DSC) ^a	287.8	292.3	291.4	292.5
A (VSM single) ^b	289	291	291	291
B (VSM ensemble) ^c	270	272	272	...

^aData from Fig. 1.

^bData from Fig. 2.

^cData from Fig. 3.

271 K in the VSM, in zero applied field. Care was taken not to overshoot the cooling. At 271 K, the magnetic field was ramped up to $\mu_0 H = 0.5$ T, with field increments of 0.05 T, and back down to zero. Following this, the field was ramped to 1 T, back to zero, to 1.5 T, and finally back to zero. Subsequently, the whole procedure was repeated while still at 271 K. Figure 4 shows how there are openings between the increasing and decreasing field branches in the first round of the procedure. In the second round, all the lines fall on top of each other, regardless of the field or direction. The sample was cooled to 266 K, heated to 271 K, and again heated to 276 K. At each temperature, the previous procedure was rerun, every time finding the same result of no hysteresis. This indicates that it is possible to gradually, but irreversibly, go from a virgin transition to a regular, symmetric one. Samples where the virgin transitions had been removed were stored under ambient conditions for up to a month before being retested with the same procedures, but the virgin transition was not reestablished.

A similar gradual procedure was devised for the DSC, as shown in Fig. 5. A single large particle of sample A with a mass of 1.66 mg was heated to 310 K and cooled to 295 K, where the cooling

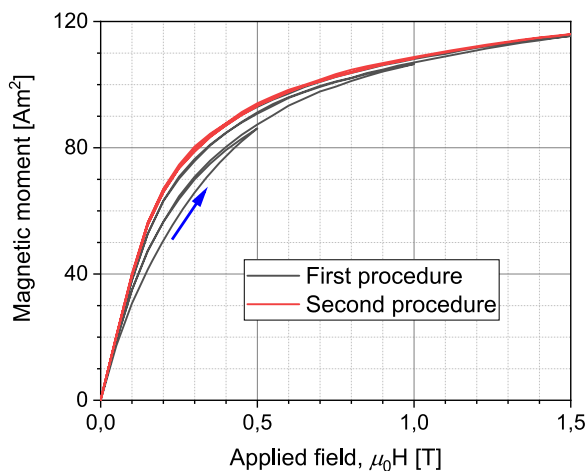


FIG. 4. VSM measurement of a single sphere of sample B obtained at 271 K after cooling from room temperature. The arrow indicates the increase in the initial direction of the field.

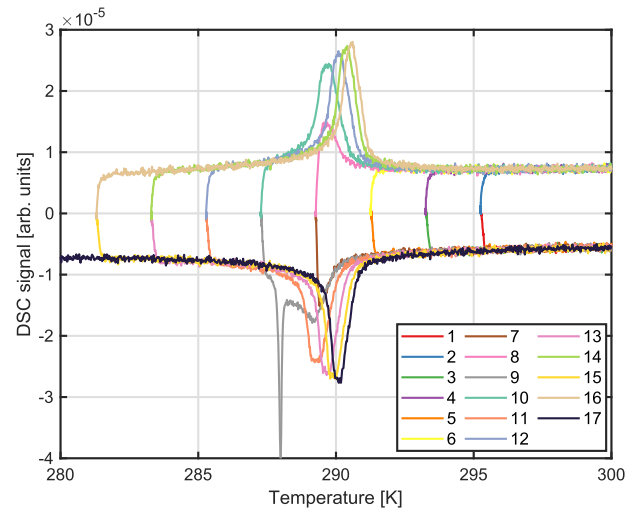


FIG. 5. Data from DSC measurements of sample A. The numbers indicate the order in which the cooling and heating measurements were conducted. The odd numbers represent cooling from 310 K, and the even ones represent heating back up to 310 K. All data are collected at a ramp rate of ± 0.5 K/min.

was stopped and the sample was heated back up to 310 K. This was repeated, going 2 K lower in each round, until 281 K. In the ninth leg of this procedure, a very sharp peak is observed at 288 K, following a smaller broad peak at about 289 K. After this leg, the expected peaks at around 290 K are observed in both the heating and cooling runs. However, it is noted that the peaks do not appear in their final sharp version until the temperature of the sample has been about 6 K below the phase transition. This again indicates a gradual, but irreversible, change from the virgin transition to the reversible normal one. From the DSC data, it is observed that the transition temperature shifts about 4.5 K per tesla of applied field. Thus, 6 K below the transition is approximately consistent with the 1.5 T applied field from the VSM experiment mentioned above.

The DSC measurements shown in Figs. 1 and 5 indicate a shift of about 2–4 K when measuring between the sharpest peak of the first and second cooling run. Similar values are found when measuring the rest of the series of alloys. In the VSM data, the shift is harder to measure as the full transition is quite broad. Values of around 1.7 K are found, with some variation from sample to sample. Due to chemical inhomogeneities in the material, there will be a variation in the transition temperature within a sphere and often more pronounced from sphere to sphere.^{21,22} The variations in both the DSC and VSM measurements are likely due to the distribution of transition temperatures present in the different samples of LaFeSi. This also explains why the transition shown in Fig. 2 is sharper than that shown in Fig. 3.

At the phase transition, $\text{La}(\text{Fe},\text{Mn},\text{Si})_{13}\text{H}_y$ experiences a volume change of about 1%.¹⁴ It seems likely that this volume increase during the first cooling will expand the structure and release some stresses entrained during the high temperature production of the materials. Scanning electron microscopy of the as-received and cycled samples was expected to reveal a change in structure and maybe cracks, which would support the idea of entrained stress.

However, no significant difference was observed between the sample before and after cooling. This may be a testament to the complexity and stability of the CALORIVAC-HS material, compared to other types of LaFeSi previously reported.^{23,24} A likely reason for this added stability is the α -Fe in the structure, which was added for this precise reason. The full series of ten materials has been operating in the magnetocaloric heat pump at DTU Energy for several months, completing tens of thousands of cycles without any structural issues.²⁵

Different production methods, particles shapes, and hydrogenation strategies have been applied since the initial discovery of the La(Fe,Si)₁₃ material family. Previous studies of the phase transition have not revealed this significant reduction in the initial transition temperature. It is, however, unclear whether this is due to the production method of the spherical particles, the inclusion of α -Fe, or some other reason.

We do not have a firm theoretical reason why this delayed normalization of the virgin transition happens. It may be due to re-distribution of the interstitial hydrogen as parts of the sample expand (when the material locally undergoes its phase transition from paramagnetic to ferromagnetic). Upon subsequent thermal cycling, the interstitial hydrogen may be distributed within the sample in a more stable configuration. The mobility of hydrogen has been previously studied in unsaturated samples of La(Fe,Mn,Si)₁₃H_y.^{26,27} Storing the samples close to the transition temperature led to a splitting of the hydrogen into two distinct distributions, observed as two peaks in the DSC data. However, the samples studied in the present work were fully saturated, so this mobility is not expected and has not been observed.

Yet another similar explanation might be found when considering re-distribution of internal stresses. As the sample cools and parts of it go through the respective transitions, the local volume expands, and this may result in a stable configuration mediated by the α -Fe phase. Validating these two suggested explanations of the observed behavior would require advanced and detailed modeling studies combining a local state function (e.g., the well-known Bean-Rodbell model²⁸) with distributions in temperature, heat transfer, local magnetic field across the sample, and structural mechanics.

From an application point of view, it is important to ensure that all materials have been cycled well below the virgin transition. Otherwise, the initially lower transition temperature may make it difficult for specific materials to create the desired temperature gradient in a device. A good example of this issue is seen in Fig. 1. Even though the transition at 290 K is very close to room temperature, the virgin temperature of about 288 K is lower than any temperature experienced in the lab or during transport. Thus, the sample has never crossed the phase transition.

Failure to cross the virgin transition of all materials before operation of a magnetocaloric device will effectively mean that the temperature spacing between individual transition temperatures will be larger than that designed, somewhere in the regenerator. This will prevent the thermal gradient in the regenerator from building up as it will have to jump further at one point than the available change in temperature. The effect of having an uneven spacing in transition temperatures is clearly observed when modeling magnetocaloric regenerators.⁵

IV. CONCLUSION

Detailed measurements of spherical La(Fe,Mn,Si)₁₃H_y particles have revealed the presence of a virgin transition, not previously reported. The virgin transition is observed as a sharp peak in the heat capacity, a few degrees below the peaks observed after cycling the samples. This sharp peak indicates an abrupt transition between the paramagnetic high temperature phase and the ferromagnetic low temperature phase. However, measurements indicate that full phase transformation is only reached after cooling about 6 K below the transition. The delayed initial transition is possibly due to the structure of the material preventing the volume expansion associated with the phase transition; however, a firm theoretical understanding remains to be established.

Importantly, for the use of La(Fe,Mn,Si)₁₃H_y in future applications, the volume change is not observed to introduce any structural damage. The lack of damage here is possibly due to the presence of α -Fe in the structure, making it more malleable.

ACKNOWLEDGMENTS

This work was, in part, financed by the RES4Build project, which received funding from the European Union's Horizon 2020 Research and Innovation Program, under Grant Agreement No. 814865.

AUTHOR DECLARATIONS

Conflict of Interest

The authors have no conflicts to disclose.

Author Contributions

Christian R. H. Bahl: Conceptualization (equal); Funding acquisition (equal); Methodology (equal); Project administration (equal); Writing – original draft (lead); Writing – review & editing (equal). **Jierong Liang:** Data curation (equal); Formal analysis (equal); Investigation (equal); Visualization (equal); Writing – review & editing (equal). **Marvin Masche:** Data curation (equal); Formal analysis (equal); Investigation (equal); Validation (equal); Writing – review & editing (equal). **Kaspar K. Nielsen:** Conceptualization (equal); Methodology (equal); Writing – review & editing (equal). **Kurt Engelbrecht:** Conceptualization (equal); Funding acquisition (equal); Methodology (equal); Writing – review & editing (equal).

DATA AVAILABILITY

The data that support the findings of this study are available from the corresponding author upon reasonable request.

REFERENCES

- 1 A. Kitanovski, J. Tušek, U. Tomc, U. Plaznik, M. Ožbolt, and A. Poredoš, *Magnetocaloric Energy Conversion* (Springer, 2016).
- 2 S. Dall'Olio, M. Masche, J. Liang, A. Insinga, D. Eriksen, R. Bjørk, K. Nielsen, A. Barcza, H. Vieyra, N. V. Beek *et al.*, "Novel design of a high efficiency multi-bed active magnetic regenerator heat pump," *Int. J. Refrig.* **132**, 243–254 (2021).

- ³J. Lyubina, "Magnetocaloric materials for energy efficient cooling," *J. Phys. D: Appl. Phys.* **50**, 053002 (2017).
- ⁴S. Jacobs, J. Auringer, A. Boeder, J. Chell, L. Komorowski, J. Leonard, S. Russek, and C. Zimm, "The performance of a large-scale rotary magnetic refrigerator," *Int. J. Refrig.* **37**, 84–91 (2014).
- ⁵T. Lei, K. K. Nielsen, K. Engelbrecht, C. R. H. Bahl, H. Neves Bez, and C. T. Veje, "Sensitivity study of multi-layer active magnetic regenerators using first order magnetocaloric material La(Fe, Mn, Si)₁₃H_y," *J. Appl. Phys.* **118**, 014903 (2015).
- ⁶C. Aprea, A. Greco, A. Maiorino, and C. Masselli, "A comparison between rare earth and transition metals working as magnetic materials in an AMR refrigerator in the room temperature range," *Appl. Therm. Eng.* **91**, 767–777 (2015).
- ⁷B. P. Vieira, H. N. Bez, M. Kuepferling, M. A. Rosa, D. Schafer, C. C. Plá Cid, H. A. Vieyra, V. Basso, J. A. Lozano, and J. R. Barbosa, Jr., "Magnetocaloric properties of spheroidal La(Fe,Mn,Si)₁₃H_y granules and their performance in epoxy-bonded active magnetic regenerators," *Appl. Therm. Eng.* **183**, 116185 (2021).
- ⁸K. Navickaitė, B. Monfared, D. Martinez, B. Palm, C. Bahl, and K. Engelbrecht, "Experimental investigation of fifteen-layer epoxy-bonded La(Fe,Mn,Si)₁₃H_y active magnetic regenerator," in *Thermag VIII-International Conference on Caloric Cooling* (International Institute of Refrigeration, 2018), pp. 84–89.
- ⁹A. Fujita, S. Fujieda, Y. Hasegawa, and K. Fukamichi, "Itinerant-electron metamagnetic transition and large magnetocaloric effects in La(Fe_xSi_{1-x})₁₃ compounds and their hydrides," *Phys. Rev. B* **67**, 104416 (2003).
- ¹⁰K. Fukamichi, A. Fujita, and S. Fujieda, "Large magnetocaloric effects and thermal transport properties of La(FeSi)₁₃ and their hydrides," *J. Alloys Compd.* **408–412**, 307–312 (2006).
- ¹¹A. Barcza, M. Katter, V. Zellmann, S. Russek, S. Jacobs, and C. Zimm, "Stability and magnetocaloric properties of sintered La(Fe,Mn,Si)₁₃H₂ alloys," *IEEE Trans. Magn.* **47**, 3391–3394 (2011).
- ¹²V. Basso, M. Kuepferling, C. Curcio, C. Bennati, A. Barcza, M. Katter, M. Bratko, E. Lovell, J. Turcaud, and L. F. Cohen, "Specific heat and entropy change at the first order phase transition of La(Fe-Mn-Si)₁₃H compounds," *J. Appl. Phys.* **118**, 053907 (2015).
- ¹³A. Waske, L. Giebler, B. Weise, A. Funk, M. Hinterstein, M. Herklotz, K. Skokov, S. Fähler, O. Gutfleisch, and J. Eckert, "Asymmetric first-order transition and interlocked particle state in magnetocaloric La(Fe,Si)₁₃," *Phys. Status Solidi RRL* **9**, 136–140 (2015).
- ¹⁴H. Neves Bez, K. K. Nielsen, A. Smith, P. Norby, K. Ståhl, and C. R. H. Bahl, "Strain development during the phase transition of La(Fe,Mn,Si)₁₃H₂," *Appl. Phys. Lett.* **109**, 051902 (2016).
- ¹⁵X. F. Miao, L. Caron, Z. Gercsi, A. Daoud-Aladine, N. H. Van Dijk, and E. Brück, "Thermal-history dependent magnetoelastic transition in (Mn,Fe)₂(P,Si)," *Appl. Phys. Lett.* **107**, 042403 (2015).
- ¹⁶M. Fries, L. Pfeuffer, E. Bruder, T. Gottschall, S. Ener, L. V. B. Diop, T. Gröb, K. P. Skokov, and O. Gutfleisch, "Microstructural and magnetic properties of Mn-Fe-P-Si (Fe₂ P-type) magnetocaloric compounds," *Acta Mater.* **132**, 222–229 (2017).
- ¹⁷A. Bartok, M. Kustov, L. F. Cohen, A. Pasko, K. Zehani, L. Bessais, F. Mazaleyrat, and M. LoBue, "Study of the first paramagnetic to ferromagnetic transition in as prepared samples of Mn-Fe-P-Si magnetocaloric compounds prepared by different synthesis routes," *J. Magn. Magn. Mater.* **400**, 333–338 (2016).
- ¹⁸J. Liang, M. Masche, K. Engelbrecht, K. K. Nielsen, H. A. Vieyra, A. Barcza, and C. R. H. Bahl, "Experimental study of non-bonded packed bed active magnetic regenerators with stabilized La(Fe,Mn,Si)₁₃H_y particles," *Appl. Therm. Eng.* **197**, 117383 (2021).
- ¹⁹K. K. Nielsen, H. N. Bez, L. von Moos, R. Bjørk, D. Eriksen, and C. R. H. Bahl, "Direct measurements of the magnetic entropy change," *Rev. Sci. Instrum.* **86**, 103903 (2015).
- ²⁰F. Erbesdobler, C. R. H. Bahl, R. Bjørk, and K. K. Nielsen, "Detailed isofield calorimetry of La(Fe,Si,Mn)H reveals distributed magnetocaloric phase transitions," *J. Appl. Phys.* **127**, 095102 (2020).
- ²¹C. Bennati, L. Gozzelino, E. S. Olivetti, and V. Basso, "Heterogeneous nucleation and heat flux avalanches in La(Fe,Si)₁₃ magnetocaloric compounds near the critical point," *Appl. Phys. Lett.* **109**, 231904 (2016).
- ²²H. N. Bez, K. K. Nielsen, P. Norby, A. Smith, and C. R. H. Bahl, "Magnetoelastic coupling in La(Fe,Mn,Si)₁₃H_y within the Bean-Rodbell model," *AIP Adv.* **6**, 056217 (2016).
- ²³J. Lyubina, R. Schäfer, N. Martin, L. Schultz, and O. Gutfleisch, "Novel design of La(Fe,Si)₁₃ alloys towards high magnetic refrigeration performance," *Adv. Mater.* **22**, 3735–3739 (2010).
- ²⁴H. N. Bez, K. Navickaitė, T. Lei, K. Engelbrecht, A. Barcza, and C. Bahl, "Epoxy-bonded La(Fe,Mn,Si)₁₃H₂ as a multi layered active magnetic regenerator," in *7th International Conference on Magnetic Refrigeration at Room Temperature (Thermag VII)* (International Institute of Refrigeration, 2016), pp. 158–163.
- ²⁵M. Masche, J. Liang, S. Dall'Olio, K. Engelbrecht, and C. R. H. Bahl, "Performance analysis of a high-efficiency multi-bed active magnetic regenerator device," *Appl. Therm. Eng.* **199**, 117569 (2021).
- ²⁶M. Krautz, J. D. Moore, K. P. Skokov, J. Liu, C. S. Teixeira, R. Schäfer, L. Schultz, and O. Gutfleisch, "Reversible solid-state hydrogen-pump driven by magnetostructural transformation in the prototype system La(Fe,Si)₁₃H_y," *J. Appl. Phys.* **112**, 083918 (2012).
- ²⁷C. B. Zimm and S. A. Jacobs, "Age splitting of the La(Fe_{1-x}Si_x)₁₃H_y first order magnetocaloric transition and its thermal restoration," *J. Appl. Phys.* **113**, 17A908 (2013).
- ²⁸C. P. Bean and D. S. Rodbell, "Magnetic disorder as a first-order phase transformation," *Phys. Rev.* **126**, 104 (1962).